Journal of Materials Chemistry C

RSC Publishing

PAPER

View Article Online
View Journal | View Issue

Programmable assembly of CdTe quantum dots into microstructures by femtosecond laser direct writing†

Cite this: *J. Mater. Chem. C*, 2013, **1**, 4699

Bin-Bin Xu,[a] Yong-Lai Zhang,*[a] Ran Zhang,[a] Lei Wang,[a] Xin-Ze Xiao,[a] Hong Xia,[a] Qi-Dai Chen[a] and Hong-Bo Sun*[ab]

Received 10th April 2013
Accepted 3rd June 2013

DOI: 10.1039/c3tc30666f

www.rsc.org/MaterialsC

Reported here is the programmable assembly of CdTe quantum dots (QDs) into various pre-designed microstructures by using a femtosecond laser direct writing (FsLDW) technique. As nanobuilding blocks, CdTe QDs could be driven by a focused femtosecond laser beam to construct arbitrarily-shaped micropatterns with high resolution (~170 nm). The optical properties of pristine CdTe QDs were well inherited after the FsLDW induced programmable assembly, which has been confirmed by the luminescence spectrum and the high resolution transmission electron microscope (HR-TEM) image of the assemblies. By using this technique, the CdTe QDs microstructures were integrated within microfluidic devices, which showed the capability of qualitative on-chip detection of heavy metal ions. The FsLDW induced assembly of QDs may open up a new way for the designable assembly of QDs towards the flexible fabrication and integration of QDs-based microdevices.

1 Introduction

Recent years have witnessed the rapidly increased research interest in semiconductor quantum dots (QDs), because of their unique optical and electronic properties, which are of great interest to a broad range of disciplines.[1–6] For instance, QDs could be used as fluorescent tags for various *in vitro* or *in vivo* biological assays.[7–9] As pivotal components, QDs hold great promise for the development of a new generation of optoelectronic devices, such as QDs sensitized solar cells (SCs) and light emitting diodes (LEDs).[4,10] The unique properties of semiconductor QDs has triggered a sustained research effort to develop novel experimental methods for allowing refined control over the size, shape, and polydispersity, as well as the assembly of QDs into hierarchical micro-nanostructures. Especially, for enhanced functionality, the rational design and precise control of the QDs assembly is of great scientific interest because the structurally-defined collective properties endow the QDs assemblies with potential applications, such as controlled plasmonic interactions,[11] optical encoding,[12] multiplex biological detection,[13] and advanced photonic devices.[14–18]

To date, with the rapid progress of classical nanofabrication methods, represented by various "bottom-up" and "top-down" approaches, semiconductor QDs, as nano-building blocks, have been successfully assembled into various micro-nanostructures.[19] For instance, QDs micro-patterns could be readily created by using pre-patterned substrates as templates which could be designed and fabricated by lithography,[20] focused ion beam pulses[21] or laser direct writing[22] beforehand. The as-formed chemical-specific micropatterns on the substrates would show special interaction with QDs, leading to the self-assmbly of QDs in a controlled manner. Recently, DNA-directed self-assembly based upon biological interactions have been successfully adopted for QDs structuring, and even the programming of their valency and assemblies.[23–25] Besides, novel strategies such as interfacial self-assembly,[26] evaporation-induced assembly,[27] postsynthesis assembly,[28] microstructuring inside the photopolymer host,[29] assembly with the help of block copolymer micelles[30] and inside a microfluidic device,[31] have also been developed for QDs assembly. More interestingly, the optical trapping technique has been used for the manipulation of individual colloidal CdSe-core QDs in three dimensions by an infrared continuous wave laser operated at low laser powers.[32] By using optical forces for positioning and the van der Waals attraction for binding them to the substrate, individual colloidal nanoparticles (NPs) with a diameter of 80 nm could be driven and printed with a positioning precision of 50 nm.[33] However, despite the recent progress in quantum-dot self-assembly and individual NPs positioning, few techniques are available for the programmable assembly of tiny QDs (*e.g.*, QDs with diameter less than 5 nm) into designed micropatterns on any desired substrate. To date, it is still challenging to fabricate

[a]*State Key Laboratory on Integrated Optoelectronics, College of Electronic Science and Engineering, Jilin University, 2699 Qianjin Street, Changchun, 130012, People's Republic of China. E-mail: yonglaizhang@jlu.edu.cn; hbsun@jlu.edu.cn; Fax: +86 431-85168281; Tel: +86 431-85168281*

[b]*College of Physics, Jilin University, 119 Jiefang Road, Changchun, 130023, People's Republic of China*

† Electronic supplementary information (ESI) available: XPS spectrum of the Pb4f region for the CdTe micropattern reacted with a Pb^{2+} solution. See DOI: 10.1039/c3tc30666f

QDs microstructures with arbitrary-shapes that permit a high level of control over the QDs distribution and their position for the purpose of designable fabrication and flexible integration of QDs-based microdevices.

As a powerful micronanofabrication technique, femtosecond laser direct writing (FsLDW) has been widely recognized as a nano-enabler for the designable fabrication of nanostructures over a wide range of materials.[34–39] Especially, for some non-periodic or complex configurations, the FsLDW technique was distinguished due to its mask-free processing capability and arbitrary-shaped designability.[35,38] In this work, we demonstrate a programmable assembly of CdTe QDs by using the FsLDW technique. With the help of an optical gradient force derived from the focused laser beam, CdTe QDs could be patterned into any desired microstructures according to the computer-designed configurations. The optical properties of pristine QDs were well inherited after the femtosecond laser induced programmable assembly. Beside, the strategy we proposed here exhibits a series of advantages (*e.g.*, mask-free, non-substrate dependence, arbitrarily-shaped and uncontacting) over traditional methods that have been reported for QDs assembly. The FsLDW induced assembly of QDs holds great promise for the fabrication and integration of QDs-based advanced microdevices.

2 Experimental

2.1 Preparation of CdTe QDs

The CdTe QDs aqueous solution was synthesized according to a modified literature method.[40] In a typical experiment, 1 mM of $CdCl_2 \cdot 2.5H_2O$ solution and 2 mM of thioglycolic acid (TGA) were mixed together, and the pH of the solution was adjusted to about 11 by the dropwise addition of NaOH solution (1 M) with stirring. Then, 0.2 mmol of NaHTe solution was added at room temperature under N_2 protection. The ratio of Cd : TGA : Te in the reaction solution was kept at 1 : 2 : 0.2. The mixture was refluxed at ~100 °C, and the desired QDs solution was obtained when its absorption peak appeared at about 460 nm.

2.2 FsLDW induced assembly of CdTe QDs

For the FsLDW, the TGA-capped CdTe quantum dots suspension was dropped onto the surface of a cover glass and the sample was placed in the femtosecond laser direct writing system (FsLDW). 800 nm femtosecond laser pulses, with a 120 fs pulse duration,[41] were tightly focused on the interface between the substrate and solution by a high numerical aperture oil-immersion objective lens (NA = 1.35, 100×). The QDs structures were fabricated by the laser scanning route which was guided by computer designed structure.

2.3 Fabrication of microfluidic devices

The PDMS-based microfluidic devices were prepared through a soft lithography technique. First, SU-8 micropatterns were fabricated by UV lithography with the help of a pre-patterned shadow mask. Then the PDMS micro-channel was prepared through soft lithography by using the SU-8 micro-pattern as a template. CdTe QDs micropattern equipped glass was used as the substrate. The gold electrodes were coated beforehand through a physical vapour deposition (PVD) process with the help of a shadow mask. For the test of Pb^{2+} detection, the CdTe QDs micropattern equipped substrate was covered with the PDMS microchannel, and pressed for adhesion. Lead nitrate was used for the preparation of Pb^{2+} aqueous solutions of different concentrations.

2.4 Characterization

The absorption spectra were measured using a Shimadzu UV-1700 spectrophotometer. The steady-state fluorescence spectra were recorded with a Shimadzu RF-5301PC spectrometer. The high resolution transmission electron microscopy (HRTEM) images were obtained with a JEOL-2100F field emission TEM. SEM images were obtained with a JEOL JSM-7500F field emission scanning electron microscope (FE-SEM) which was equipped with JSM 7001F energy dispersive X-ray analysis (EDS) for materials analysis division. X-ray photoelectron spectroscopy (XPS) was performed using an ESCALAB 250 spectrometer. The photographs of the QDs structures were taken by using widefield fluorescence microscopy on a BK-FL4 fluorescence microscope.

3 Results and discussion

In our work, TGA-capped CdTe QDs in aqueous solution were chosen as a representative example for the FsLDW induced programmable assembly of semiconductor QDs. In a typical procedure, the CdTe QDs suspension was dropped onto a cover glass which was placed on the piezo moving stage of the laser processing system, as shown in Fig. 1. In our previous work, we reported the successful assembly of gold nanoparticles due to the optical forces induced deposition and aggregation in the laser focused area.[42] In this work, the optical trapping technique has been used for the programmable assembly of semiconductor QDs through a FsLDW process. The optical trapping forces exerted on the QDs generally include absorption force, scattering force and gradient force.[43,44] Note that the size of the QDs is only a few nanometers, the scattering and absorption forces are negligible, thus the gradient force was the dominant

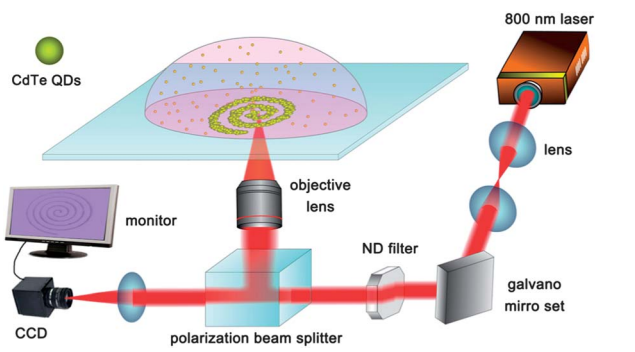

Fig. 1 Schematic illustration for the femtosecond laser direct writing induced programmable assembly of CdTe QDs.

factor. During the FsLDW process, controlled amounts of momentum were applied to the QDs, which expelled them from the colloidal suspension and deposited them on the designated site of the substrate. Here, the optical gradient force plays the role in driving the QDs assembly according to the laser scanning track, and the laser irradiation induced heat effect would cause the partial aggregation of QDs, forming pre-designed microstructures after removal of the residual QDs solutions. It is important to point out that the femtosecond laser pulse was critical for the QDs patterning, because the ultrafast pulse ranging from tens to hundreds of femtoseconds can effectively suppress the thermal relaxation processes which occurs on a timescale of hundreds of nanoseconds. Only if the heat provided by laser irradiation is not sufficient enough to cause the formation of CdTe bulky crystal, could the resultant microstructure be considered as the assembly of QDs.

Taking advantage of the designable fabrication capability of FsLDW, the CdTe QDs could be programmably assembled into various microstructures. Fig. 2 shows different CdTe QDs micropatterns fabricated on the surface of glass slices. A luminescence microscopic image of the as-fabricated CdTe QDs micro-circle shows that their luminescence is strong enough to be observed by luminescence microscopy under excitation, indicating the inheritance of optical properties from pristine CdTe QDs. As the FsLDW technique was commanded by computer-designed microstructures, the CdTe QDs could be assembled into various complex configurations, such as the badge of Jilin university and even the effigy of *Albert Einstein* (Fig. 2b–e). By patterning the CdTe QDs into a spiral circle microstructure, we evaluated the dependence of fabrication resolution (represented by line width) on the laser power. With the increase of laser power from 10 mW to 45 mW, the line width of the resultant CdTe QDs structure increases from ~170 nm to ~1.75 μm (Fig. 2f). In our work, the thinnest line width was ~170 nm when the laser power was 10 mW (Fig. 2c), further decrease of the line width by using a lower laser power would result in discontinuous lines or poor reproducibility. This dependence was on account of the combinative nonlinear effect of light-matter interactions and the threshold response of the aggregation of QDs, which is similar to that in two-photon photopolymerization (TPP).[36] According to our results, laser powers ranging from 10 mW to 40 mW were considered to be appropriate processing conditions for CdTe QDs patterning. The fabrication under a too large laser intensity would lead to the growth of CdTe crystals, whereas a too low laser power would result in discontinuous microstructures or failure to assemble.

The UV-vis absorption and luminescence spectra of both the pristine CdTe QDs and the CdTe QDs assemblies are shown in Fig. 3. Compared with the pristine QDs, an obvious red-shift could be observed in both the absorption and luminescence spectra of the QDs assemblies. This could be attributed to the decrease of the confinement effect in the assemblies and the loss of the surface-capping ligands during the femtosecond laser induced aggregation. Moreover, during the laser induced aggregation, the dipole–dipole coupling interactions would happen between neighboring QDs, which could also give rise to the red-shift of the PL. These results indicate that the steady state optical properties of the QDs were well inherited after the programmable assembly. Although the QDs have been used as nanobuilding blocks in the large assemblies, the quantum confinement properties are still in effect, a similar phenomenon could also be found in QD-based mesocrystals.[45]

To get further insight into the crystalline structure of the CdTe QDs assemblies, the sample was investigated by high resolution transmission electron microscopy (HR-TEM). No

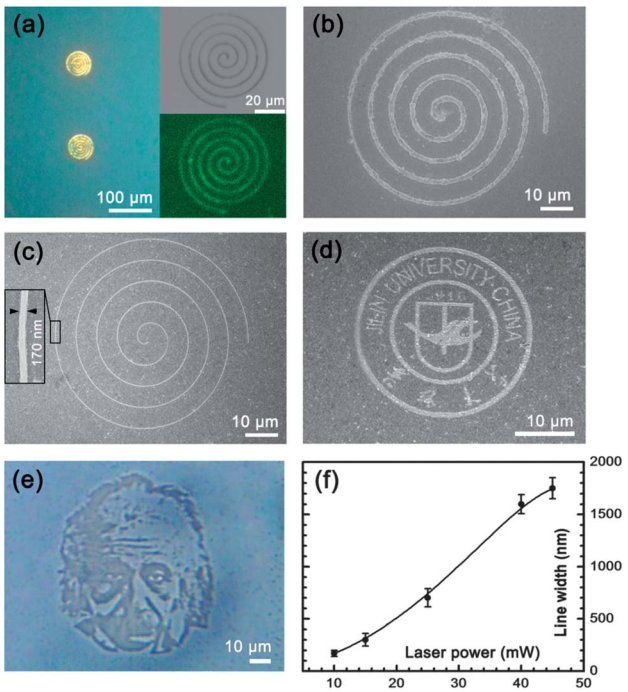

Fig. 2 Morphologies of CdTe QDs micropatterns. (a) A luminescence microscopic image of the CdTe QDs microstructures, the insets are the microscopic image and confocal microscopic images of the circle structure; (b and c) SEM image of CdTe QDs micro-circles with different line widths; (d) SEM image of the badge of Jilin University; (e) Optical microscopic image of the CdTe QDs micro-pattern, the effigy of *Albert Einstein*; (f) Dependence of line width on laser power.

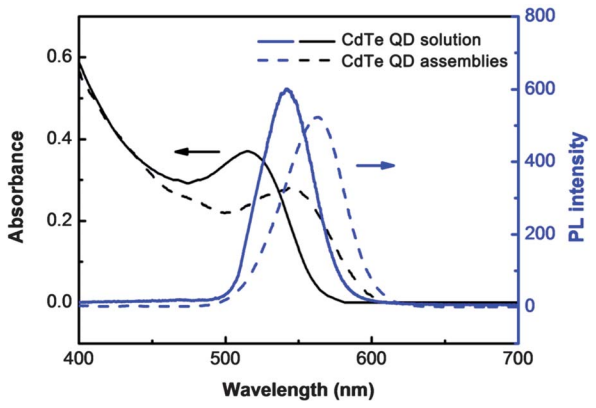

Fig. 3 Absorption (black lines) and luminescence spectra (blue lines) of CdTe QDs (solid lines) and CdTe QDs assemblies (dashed lines). An obvious red-shift could be observed in both the absorption and luminescence spectra of the assembly sample compared with the pristine CdTe QDs.

bulky single crystal could be observed over all of the sample. On the contrary, the assemblies consisting of individual nanocrystals (yellow circle) with an average size of ~4 nm, are in good agreement with the size of the pristine CdTe QDs. As shown in Fig. 4, the lattice spacing of the building units was 3.75 Å and 3.52 Å, which corresponds to the (002) and (101) planes in the hexagonal phase of CdTe, respectively. These results directly provide the evidence that the CdTe QDs serve as nanobuilding blocks in the FsLDW induced assembly, instead of the material source for the formation of CdTe bulky crystals.

As fluorescent probes, semiconductor QDs have exhibited great potential for the highly sensitive detection of heavy metal ions, such as Pb^{2+} and Hg^{2+}.[46] However, the presence of toxic elements (*e.g.*, Cd, Pb) in the semiconductor QDs significantly restricts their practical applications.[47] In our work, we integrated the CdTe QDs micropatterns within a microfluidic device which was further used for the on-chip detection of heavy metal ions. As a representative target ion, Pb^{2+} aqueous solution (0.1 M, lead nitrate) was injected into the microfluidic channel for the on-chip detection and an obvious luminescence quenching could be observed. Here, we did not pursue the high sensitivity and low detection limit, as the assembly of QDs would significantly decrease their surface area as compared with monodisperse QDs. The major advantages of the integration of CdTe QDs microstructures within a microfluidic chips lies in the immobilization of the toxic CdTe QDs and the high-throughput detection by means of microfluidic techniques. Moreover, taking advantage of the flexible patterning property, the QDs structures could be designed and fabricated according to the shape of the microchannels. For the purpose of achieving a better sensing performance, QDs microstructures with larger exposed surfaces could be readily fabricated.

In this work, a PDMS microfluidic channel prepared by soft lithography was covered on a glass substrate with pre-patterned CdTe QDs microstructures. As shown in Fig. 5a, to monitor the conductivity change in the presence of Pb^{2+}, we also coated two gold electrodes to connect the CdTe QDs microline arrays. Before the injection of the Pb^{2+} solution, the CdTe QDs microline arrays could be clearly recognized from a luminescence microscopic image (middle image of Fig. 5b). However, after immersing in Pb^{2+} solution for a few minutes, the luminescence was quenched drastically (right image of Fig. 5b), indicating the qualitative sensing performance. Besides, we also tested the conductivity change before and after the Pb^{2+} quenching of PL, as shown in Fig. 5c, the conductivity of the pristine CdTe QDs micro-lines were very low, almost insulating. However, after the addition of Pb^{2+} (0.1 M) for only 1 min, the resistance decreased obviously (~7.5 MΩ). Further extending the reaction time did not show an obvious influence on the conductivity, which indicates the reaction occurs within 1 min. Despite the Pb^{2+} induced resistance change not being reversible, which limited its application as a resistance-based ion sensing device, it

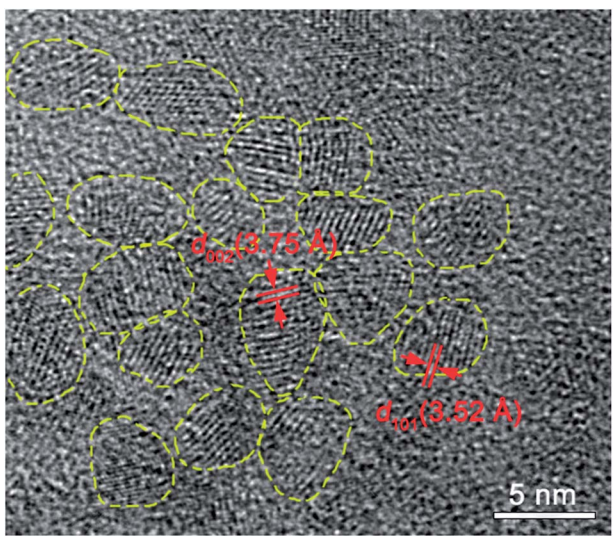

Fig. 4 High-resolution TEM image of the CdTe QDs assembly sample, the yellow circles indicate individual nanocrystals.

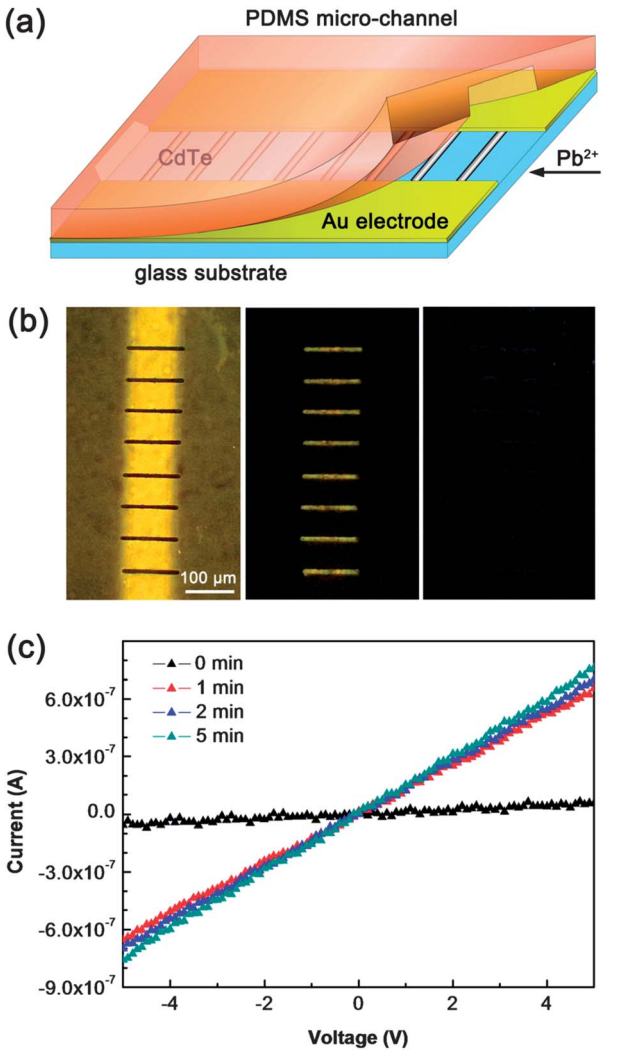

Fig. 5 (a) Scheme of the PDMS microfluidic channel; (b) Optical microscopic image and luminescence microscopic images of the CdTe micro-line arrays between the two gold electrodes (from left: optical image, luminescence image, and luminescence image in the presence of Pb^{2+}); (c) *I–V* curves of the CdTe QDs micro-lines between the Au electrodes and after immergence in Pb^{2+} solution for different lengths of time.

provides a new method for the *in situ* monitoring of Pb^{2+} detection in addition to the luminescence spectroscopy.

To get further insight into the luminescence quenching mechanism in the presence of Pb^{2+}, we investigated the CdTe QDs microstructure by elemental maps. Fig. 6a shows the SEM image of the CdTe QDs micro-circle arrays with different line widths fabricated on the substrate of a microfluidic device. After the immergence in Pb^{2+} solution, Cd, Te, and Pb elements were detected. As shown in Fig. 6b, in addition to Si element, which mainly derived from the glass substrate, Cd, Te and Pb were homogeneously distributed over the micro-pattern. The maps of these elements not only confirm that the pattern consisted of CdTe QDs, but also indicates the homogeneous distribution of Pb^{2+} ions. XPS spectrum of the Pb4f region for the CdTe micropattern reacted with a Pb^{2+} solution shows that primary Pb4f peaks recorded at 138.8 eV ($4f_{7/2}$) and 143.7 eV ($4f_{5/2}$) could be attributed to Pb(II),[48] indicating no chemical reduction of Pb^{2+} occurs on the surface of the CdTe micropattern (ESI†). As reported elsewhere,[49,50] the competitive binding of capped thio-groups between the QDs and Pb^{2+} results in the changes in surface and photophysical properties of the QDs, leading to PL quenching. Providing that the mercapto groups of the capped molecules play a critical role in the Pb^{2+} sensing,[49] CdTe QDs capped with glutathione (GSH) and mercapto propionic acid (MPA) may also show similar properties.

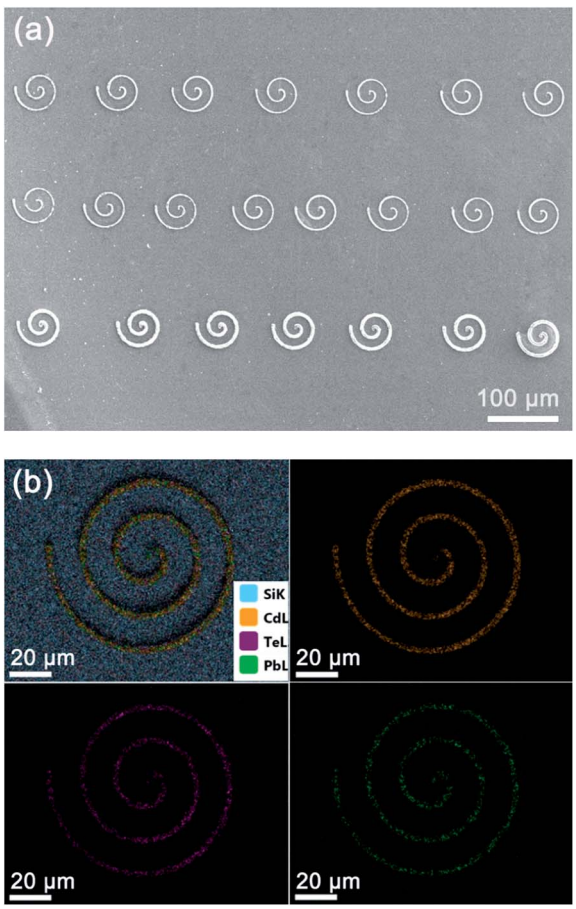

Fig. 6 (a) SEM image of the CdTe QDs micro-circle arrays; (b) Cd, Te, Pb elemental maps of a single CdTe QDs micro-circle after the immergence in Pb^{2+} solution.

4 Conclusions

In conclusion, a programmable assembly of CdTe QDs has been successfully developed using the FsLDW technique. As representative examples, microstructures including a spiral micro-circle, the badge of Jilin University and even the effigy of *Albert Einstein* were readily fabricated. The resolution of the QDs microstructures shows a certain dependence on the femtosecond laser power, and the highest resolution was achieved at ~170 nm. The luminescence spectrum and the HR-TEM image of the QDs assemblies gives the evidence that the obtained microstructures consist of CdTe QDs. No bulky crystal was observed due to the use of ultrafast femtosecond laser pulse which can effectively suppress the thermal relaxation processes, and therefore, avoid the heat induced growth of nanocrystals. The optical properties of pristine CdTe QDs have been well inherited after the FsLDW induced programmable assembly. The CdTe QDs microstructures could be readily fabricated within given microdevices, such as microfluidic chips, in this case it could be used for the qualitative on-chip detection of heavy metal ions. The reported method may find broad applications in the flexible integration of QDs-based microdevices.

Acknowledgements

We acknowledge Xue-Qing Liu, Lei Wang, Bing Han, and Chao Lv for the help of sample characterization and the useful discussion on this paper. This work is supported by the National Science Foundation of China (Grant nos 90923037, 61008014 and 6078048). We also acknowledge the China Postdoctoral Science Foundation no. 20110490156 and the Hong Kong Scholar Program XJ2011014. The work was also supported by 2012 PhD interdisciplinary project no. 450060483105, Jilin University.

Notes and references

1 R. Gill, M. Zayats and I. Willner, *Angew. Chem., Int. Ed.*, 2008, **47**, 7602–7625.
2 P. V. Kamat, *J. Phys. Chem. C*, 2008, **112**, 18737–18753.
3 D. J. Mowbray and M. S. Skolnick, *J. Phys. D: Appl. Phys.*, 2005, **38**, 2059–2076.
4 A. J. Nozik, M. C. Beard, J. M. Luther, M. Law, R. J. Ellingson and J. C. Johnson, *Chem. Rev.*, 2010, **110**, 6873–6890.
5 K. E. Sapsford, T. Pons, I. L. Medintz and H. Mattoussi, *Sensors*, 2006, **6**, 925–953.
6 D. Vanmaekelbergh and P. Liljeroth, *Chem. Soc. Rev.*, 2005, **34**, 299–312.
7 C. Wang, X. Gao and X. G. Su, *Anal. Bioanal. Chem.*, 2010, **397**, 1397–1415.
8 D. W. Deng, Y. Q. Chen, J. Cao, J. M. Tian, Z. Y. Qian, S. Achilefu and Y. Q. Gu, *Chem. Mater.*, 2012, **24**, 3029–3037.
9 H. Mattoussi, G. Palui and H. B. Na, *Adv. Drug Delivery Rev.*, 2012, **64**, 138–166.

10 H. V. Demir, U. O. S. Seker, G. Zengin, E. Mutlugun, E. Sari, C. Tamerler and M. Sarikaya, *ACS Nano*, 2011, **5**, 2735–2741.
11 S. L. Westcott, S. J. Oldenburg, T. R. Lee and N. J. Halas, *Chem. Phys. Lett.*, 1999, **300**, 651–655.
12 J. Yang, S. R. Dave and X. H. Gao, *J. Am. Chem. Soc.*, 2008, **130**, 5286–5292.
13 F. Y. Song, P. S. Tang, H. Durst, D. T. Cramb and W. C. W. Chan, *Angew. Chem., Int. Ed.*, 2012, **51**, 8773–8777.
14 K. K. Jang, P. Prabhakaran, D. Chandran, J. J. Park and K. S. Lee, *Opt. Mater. Express*, 2012, **2**, 519–525.
15 K. S. Lee, P. N. Prasad, G. Huyet and C. H. Tan, *Opt. Express*, 2012, **20**, 10721–10723.
16 K. S. Lee, P. N. Prasad, G. Huyet and C. H. Tan, *Opt. Mater. Express*, 2012, **2**, 682–684.
17 P. Prabhakaran, W. J. Kim, K. S. Lee and P. N. Prasad, *Opt. Mater. Express*, 2012, **2**, 578–593.
18 T. Bhuvana, B. Kim, X. Yang, H. Shin and E. Kim, *Angew. Chem., Int. Ed.*, 2013, **52**, 1180–1184.
19 I. U. Arachchige and S. L. Brock, *Acc. Chem. Res.*, 2007, **40**, 801–809.
20 M. Junkin, J. Watson, J. P. V. Geest and P. K. Wong, *Adv. Mater.*, 2009, **21**, 1247.
21 M. Gherasimova, R. Hull, M. C. Reuter and F. M. Ross, *Appl. Phys. Lett.*, 2008, **93**, 023106.
22 C. Wu, Y. S. Wang, X. M. Y. Han, X. M. Hu, Q. Y. Cheng, B. H. Han, Q. Liu, T. L. Ren, Y. H. He, S. Q. Sun and H. Ma, *Nanotechnology*, 2012, **23**, 235302.
23 J. Sharma, Y. G. Ke, C. X. Lin, R. Chhabra, Q. B. Wang, J. Nangreave, Y. Liu and H. Yan, *Angew. Chem., Int. Ed.*, 2008, **47**, 5157–5159.
24 Z. T. Deng, A. Samanta, J. Nangreave, H. Yan and Y. Liu, *J. Am. Chem. Soc.*, 2012, **134**, 17424–17427.
25 G. Tikhomirov, S. Hoogland, P. E. Lee, A. Fischer, E. H. Sargent and S. O. Kelley, *Nat. Nanotechnol.*, 2011, **6**, 485–490.
26 S. Y. Yang, C. F. Wang and S. Chen, *J. Am. Chem. Soc.*, 2011, **133**, 8412–8415.
27 J. X. Chen, W. S. Liao, X. Chen, T. L. Yang, S. E. Wark, D. H. Son, J. D. Batteas and P. S. Cremer, *ACS Nano*, 2009, **3**, 173–180.
28 H. Zhang, K. Cheng, Y. M. Hou, Z. Fang, Z. X. Pan, W. J. Wu, J. L. Hua and X. H. Zhong, *Chem. Commun.*, 2012, **48**, 11235–11237.
29 J. J. Park, P. Prabhakaran, K. K. Jang, Y. Lee, J. Lee, K. Lee, J. Hur, J. M. Kim, N. Cho, Y. Son, D. Y. Yang and K. S. Lee, *Nano Lett.*, 2010, **10**, 2310–2317.
30 M. F. Wang, M. Zhang, J. Li, S. Kumar, G. C. Walker, G. D. Scholes and M. A. Winnik, *ACS Appl. Mater. Interfaces*, 2010, **2**, 3160–3169.
31 G. Schabas, H. Yusuf, M. G. Moffitt and D. Sinton, *Langmuir*, 2008, **24**, 637–643.
32 L. Jauffred, A. C. Richardson and L. B. Oddershede, *Nano Lett.*, 2008, **8**, 3376–3380.
33 A. S. Urban, A. A. Lutich, F. D. Stefani and J. Feldmann, *Nano Lett.*, 2010, **10**, 4794–4798.
34 L. Guo, R. Q. Shao, Y. L. Zhang, H. B. Jiang, X. B. Li, S. Y. Xie, B. B. Xu, Q. D. Chen, J. F. Song and H. B. Sun, *J. Phys. Chem. C*, 2012, **116**, 3594–3599.
35 S. H. Park, D. Y. Yang and K. S. Lee, *Laser Photonics Rev.*, 2009, **3**, 1–11.
36 Y. Tian, Y. L. Zhang, J. F. Ku, Y. He, B. B. Xu, Q. D. Chen, H. Xia and H. B. Sun, *Lab Chip*, 2010, **10**, 2902–2905.
37 B. B. Xu, R. Zhang, X. Q. Liu, H. Wang, Y. L. Zhang, H. B. Jiang, L. Wang, Z. C. Ma, J. F. Ku, F. S. Xiao and H. B. Sun, *Chem. Commun.*, 2012, **48**, 1680–1682.
38 Y. L. Zhang, Q. D. Chen, H. Xia and H. B. Sun, *Nano Today*, 2010, **5**, 435–448.
39 Y. L. Zhang, L. Guo, S. Wei, Y. Y. He, H. Xia, Q. D. Chen, H. B. Sun and F. S. Xiao, *Nano Today*, 2010, **5**, 15–20.
40 Z. Y. Gu, L. Zou, Z. Fang, W. H. Zhu and X. H. Zhong, *Nanotechnology*, 2008, **19**, 135604.
41 H. B. Sun and S. Kawata, *Adv. Polym. Sci.*, 2004, **170**, 169.
42 B. B. Xu, R. Zhang, H. Wang, X. Q. Liu, L. Wang, Z. C. Ma, Q. D. Chen, X. Z. Xiao, B. Han and H. B. Sun, *Nanoscale*, 2012, **4**, 6955–6958.
43 L. Jauffred and L. B. Oddershede, *Nano Lett.*, 2010, **10**, 1927–1930.
44 L. Jauffred, A. C. Richardson and L. B. Oddershede, *Nano Lett.*, 2008, **8**, 3376–3380.
45 H. J. Chen, V. Lesnyak, N. C. Bigall, N. Gaponik and A. Eychmuller, *Chem. Mater.*, 2010, **22**, 2309–2314.
46 H. M. Wu, J. G. Liang and H. Y. Han, *Microchim. Acta*, 2008, **161**, 81–86.
47 Y. B. Zhang, W. Chen, J. Zhang, J. Liu, G. P. Chen and C. Pope, *J. Nanosci. Nanotechnol.*, 2007, **7**, 497–503.
48 M. Bonato, K. V. Ragnarsdottir and G. C. Allen, *Water, Air, Soil Pollut.*, 2012, **223**, 3845–3857.
49 E. M. Ali, Y. G. Zheng, H. H. Yu and J. Y. Ying, *Anal. Chem.*, 2007, **79**, 9452–9458.
50 W. Y. Zhong, C. Zhang, Q. Gao and H. Li, *Microchim. Acta*, 2012, **176**, 101–107.

